

# Behavior of Aspartic Acid as a Corrosion Inhibitor for Steel<sup>\*</sup>

D.J. Kalota and D.C. Silverman<sup>\*</sup>

## ABSTRACT

*Corrosion inhibition of steel by aspartic acid ( $C_4H_7NO_4$ ), an amino acid of low molecular weight, was found to depend strongly on pH. At a pH less than the ionization constant at ~ 9.5 to 10 (measured at 25°C),  $C_4H_7NO_4$  appeared to accelerate corrosion. Above that pH, it acted as a corrosion inhibitor for steel. A specially constructed potential-pH diagram for iron (Fe) that incorporated  $C_4H_7NO_4$  showed the change in behavior was accompanied by the most stable thermodynamic state changing from an iron aspartate complex to iron oxide. Polymerized  $C_4H_7NO_4$  (polyaspartic acid) behaved in a similar manner. Some other amino acids of low molecular weight behaved similarly.*

**KEY WORDS:** amino acid, aspartic acid, corrosion, inhibition, electrochemical impedance spectroscopy, iron, pH, polyaspartic acid, potential-pH diagrams, Pourbaix diagram, rotating cylinder electrode, steel

## INTRODUCTION

Corrosion inhibitors for steel continue to be developed and characterized because of the ubiquitous use of steel in construction and its somewhat limited corrosion resistance, especially in the presence of water. Amino acids have aroused periodic interest as corrosion inhibitors in recent years. One reason for that interest is that environmental restrictions are being placed on a number of common inorganic corrosion inhibitors

(i.e., chromates).<sup>1</sup> Alternatives are required. Amino acids would be biodegradable and might accommodate at least some of the environmental restrictions if they could be shown effective as corrosion inhibitors.

Several recent studies have suggested at least some of the amino acids can function as corrosion inhibitors for iron (Fe) and steel. Hluchan, Wheeler, and Hackerman<sup>2</sup> examined 22 amino acids as potential corrosion inhibitors for Fe in strong acid (1 M hydrochloric acid [HCl]). They found corrosion inhibition increased with increases in the length of the hydrocarbon chain or the number of additional amino groups. However, the shorter-chain amino acids such as glycine ( $C_2H_5O_2N$ ), aspartic acid ( $C_4H_7NO_4$ ), and glutamic acid ( $C_5H_9O_4N$ ) showed only ~ 50% reduction in corrosion rate as estimated by corrosion currents. Such a small decrease in corrosion current probably would not be of practical use at that pH.

One important application area is the corrosion inhibition of steel during containment and transport of aqueous solutions at nearly neutral pH ( $5 < \text{pH} < 9$ ). Ramakrishnaiah examined corrosion characteristics of a number of amino acids and other organic acids in sodium chloride (NaCl) solutions at pH = 8.<sup>3</sup> The goal was to examine the effects of biological compounds that might interact with steel when bacteria, algae, and fungi were present. While some amino acids decreased corrosion, others (i.e.,  $C_4H_7NO_4$ ) seemed to accelerate corrosion. In no case was the corrosion rate reduced sufficiently that any of the amino acids could serve as a practical corrosion inhibitor.

<sup>\*</sup> Submitted for publication May 1993.

<sup>\*</sup> Monsanto Co., 800 N. Lindbergh Blvd., St. Louis, MO 63167.

In a recent patent, various amino acids and their salts were found to prevent the atmospheric corrosion of Fe panels at very high concentrations.<sup>4</sup> The panels were dipped in solutions containing ~ 20 wt% of the amino acid and then hung indoors. No corrosion was observed. Atmospheric condensate would be expected to have a slightly acidic pH near 5.5.<sup>5</sup> Though the amino acid concentration was much higher than the 100 ppm in Ramakrishnaiah's study, the difference in results suggested pH might play a significant role in the ability of at least some amino acids to affect corrosion. This influence also was suggested by the fact that the amino acids had more than one acid-base constant. For example, in the case of  $C_4H_7NO_4$ , there are three pK values, indicating the molecule could have any one of four charges as a function of pH: +1, 0, -1, or -2, with the charge becoming more negative as pH increased.<sup>6</sup>

The objective of the present work was to study the effect of pH on the corrosion inhibition of Fe by low molecular weight, dicarboxylic amino acids, focusing on  $C_4H_7NO_4$  as the model compound. The pH region of interest was ~ 8 through 12.<sup>7</sup>

Potential-pH diagrams were used to establish if and over what pH and potential ranges iron-aspartate complexes theoretically would be stable. A combination of electrochemical impedance spectroscopy (EIS), the rotating cylinder electrode (RCE), and coupon immersion tests were used to estimate the corrosion rate of steel in the presence of  $C_4H_7NO_4$ .

## EXPERIMENTAL

Steel (UNS G10180)<sup>(1)</sup> was used for all experiments. The EIS apparatus, the algorithm for generating the impedance spectra, the algorithm for analyzing the results, the RCE apparatus, and the electrode geometry have been described in detail previously.<sup>8-10</sup> The electrodes were presanded using 600-grit silicon carbide (SiC) paper. The impedance spectra were generated for steel in 1,000 ppm by weight ( $7.5 \times 10^{-3}$  M) sodium aspartate periodically over an exposure period of 24 h at a pH of 8 and over 48 h at a pH of 10 and 12. The pH was adjusted using reagent-grade sodium hydroxide (NaOH). The  $C_4H_7NO_4$  used was food-grade as manufactured. In addition, impedance spectra were generated for steel in the absence of  $C_4H_7NO_4$  at pH = 10. The conductivity was adjusted to that of the solutions containing  $C_4H_7NO_4$  using sodium sulfate ( $Na_2SO_4$ ). All spectra were generated at 90°C at 200 rpm and 1,000 rpm to

examine the effect of fluid motion. The electrode was kept at 200 rpm during the entire experiment except for 1-h excursions to 1,000 rpm each day.

Immersion tests were performed in ~ 750 cc of solution in glass vessels in which rectangular steel specimens (coupons) were hung. Coupons were presanded using 120-grit SiC paper. Water-saturated air flowed through all of the vessels. The immersion experiments lasted ~ 168 h. The jars were placed in a constant-temperature bath. Two temperatures, 30°C and 90°C, were used for all experiments. The pH was adjusted at room temperature to the appropriate level using NaOH. Duplicate exposures were run in many cases. The pH was measured at room temperature and at 90°C.

## POTENTIAL-PH DIAGRAMS

Potential-pH diagrams were developed for Fe in the presence of  $C_4H_7NO_4$  to explore if formation of adducts of Fe and aspartate would be favorable thermodynamically. If an iron-aspartate complex appeared on a potential-pH diagram, the suggestion would be that an adduct of the two species would provide an additional reaction pathway. However, the presence of the species would not necessarily indicate corrosion was enhanced. If the species adhered to or reacted with the Fe surface, corrosion inhibition might result.

Previous work has suggested that iminodiacetic acid (IDA) can form a stable, soluble complex with Fe that could accelerate corrosion of steel in the near-neutral and slightly basic pH range.<sup>11</sup>  $C_4H_7NO_4$  and IDA have the same functional groups but are arranged differently. IDA has two acetic acid moieties connected to a nitrogen (N), but  $C_4H_7NO_4$  has an acetic acid moiety and a carboxylic acid group connected to a carbon (C) atom that itself has an amine group connected to it. Each molecule has two carboxylic acid groups and one amine group. Both molecules might be expected to have similar stability constants and an  $C_4H_7NO_4$ -Fe adduct might also affect the corrosion of steel.

The potential-pH diagrams were developed following the procedure outlined previously for incorporating organic complexing agents in these diagrams.<sup>11</sup>  $C_4H_7NO_4$  was created in a virtual state of 1 atm (298K) from its elemental constituents. The molecule was then introduced into water at 1 molal concentration, unit activity coefficient. The pK values for the various acid-base constants of  $C_4H_7NO_4$  were used to estimate the free energies of formation of the various aspartate species. Finally, reported stability constants for Fe and ferric aspartate were used to estimate the free energies of formation of these species.<sup>12-14</sup> Three dissolved iron-aspartate adducts

<sup>(1)</sup> UNS numbers are listed in *Metals and Alloys in the Unified Numbering System*, published by the Society of Automotive Engineers (SAE) and cosponsored by ASTM.



**FIGURE 1.** Potential-pH diagram for Fe in the presence of  $C_4H_7NO_4$  at  $90^\circ C$ , aspartate at  $7.5 \times 10^{-3}$  activity, all other ions at  $10^{-6}$  activity: (a) solid species diagram and (b) dissolved species diagram.  $\Delta$  = pH and  $E_{corr}$  for Fe in the presence of aspartate.

were included: Fe(II)-aspartate, Fe(II)-(aspartate) $_2^{-2}$ , and Fe(III)-aspartate $^+$ .

Figure 1(a) shows the solid species portion of the potential-pH diagram for Fe in the presence of  $C_4H_7NO_4$  at  $90^\circ C$ . Figure 1(b) shows the dissolved species diagram. The total potential-pH diagram (or Pourbaix diagram) is the overlay of the two.<sup>15</sup> Only the pH range greater than the middle acid-base pK is shown. The two  $C_4H_7NO_4$  species linked by an acid-base reaction were assumed to be in equilibrium at the pH equal to the pK of that reaction. All inorganic dissolved Fe species were at  $10^{-6}$  activity while the iron aspartate and  $C_4H_7NO_4$  species were at  $7.5 \times 10^{-3}$  activity. The diagram at  $25^\circ C$  was similar to that at  $90^\circ C$ . The major feature was the presence of a wide

region of stability of the complex (Fe(II)-(aspartate) $_2$ ) $^{-2}$  on the solid species diagram in place of magnetite ( $Fe_3O_4$ ), hematite ( $Fe_2O_3$ ), and solid ferric hydroxide [ $Fe(OH)_2$ ].<sup>16</sup> The pK values were corrected for temperature, assuming that the enthalpy and entropy change for the  $C_4H_7NO_4$  ionization was the same as for IDA ionization for which some data exist.<sup>6</sup> The agreement of the intersection of species boundaries at the highest pK (pH = 8.4 at  $90^\circ C$ ) strongly suggested the estimates were reasonable. The value of 8.4 also agreed with pH values measured at the temperature discussed later. At a pH of 8 ( $25^\circ C$ ) at which  $C_4H_7NO_4$  was found to be a corrosion accelerator,<sup>3</sup> an adduct with Fe was the most stable species.

However, the most basic pK for  $C_4H_7NO_4$  has a value of  $\sim 9.65$  at  $25^\circ C$ , which was estimated to be  $\sim 8.4$  at  $90^\circ C$ . The question was whether the iron-aspartate complex was the expected product above and below this pH. There might be a change in behavior at a pH above and below this constant. Experiments were conducted to investigate the corrosion characteristics between pH 8 and 12.

## EXPERIMENTAL RESULTS

### RCE

Figures 2 through 4 show the EIS spectra for steel in the presence of  $7.5 \times 10^{-3} M$  (1,000 ppm by weight)  $C_4H_7NO_4$  adjusted to a pH of 8 and 10 and in the absence of  $C_4H_7NO_4$ , also at a pH of 10. The spectra generated at 200 rpm after  $\sim 24$  h of exposure are shown. The spectra at a pH of 8 in the presence of  $C_4H_7NO_4$  and at a pH of 10 in the absence of  $C_4H_7NO_4$  were fitted by using one relaxation time constant and one constant phase element. The spectra at a pH of 10 and 12 (not shown) were fitted using a nested combination of two relaxation time constants and two constant phase elements. The circuits used have been described previously.<sup>10</sup>

Figure 5 shows a plot of the reciprocal of the resistance ( $R_p$ ) assumed to be related to the corrosion rate as a function of time and rotation rate. This type of plot shows how the corrosion rate changes with time and the relationship among the corrosion rates.<sup>10</sup> The resistance associated with the low frequency relaxation time constants at pH values of 10 and 12 were assumed to be related to the corrosion rate. The resistance associated with the single time constant for the case of a pH of 8 and for the case of pH of 10 without  $C_4H_7NO_4$  were assumed to be related to the corrosion rate.

Table 1 shows the time-averaged corrosion rate estimated from the impedance spectra compared to the corrosion rate estimated from a mass lost by the electrode. A Tafel constant of 0.025 V was used for all cases. Agreement was reasonable. If the resistance associated with the high frequency relaxation time constant at a pH of 10 and 12 had been used, the estimated corrosion rate would have been  $\sim 2$  orders of magnitude greater because those resistances were  $\sim 2$  orders of magnitude smaller.

### Immersion Experiments

Table 2 shows results of the immersion experiments at  $30^\circ C$ . Table 3 shows results for the immersions as a function of concentration and pH at  $90^\circ C$ . Most of the effort was concentrated at the higher temperature. Results in Table 3 show the effects of concentration and pH on corrosion rate and appearance of the steel.

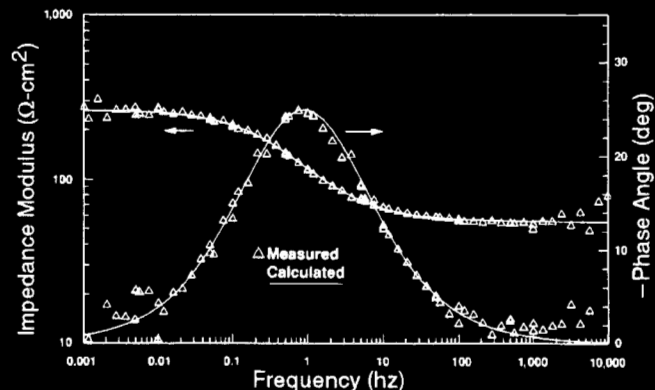


FIGURE 2. Impedance spectrum of steel in the absence of aspartate ion at  $90^\circ C$ , pH = 10, and 200 rpm after 24 h of exposure (Bode format).

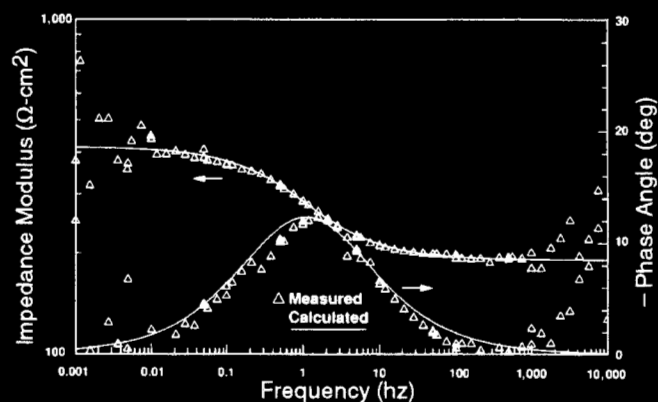


FIGURE 3. Impedance spectrum of steel in solution containing  $7.5 \times 10^{-3} M$  aspartate ion at  $90^\circ C$ , pH = 8, and 200 rpm after 24 h of exposure (Bode format).

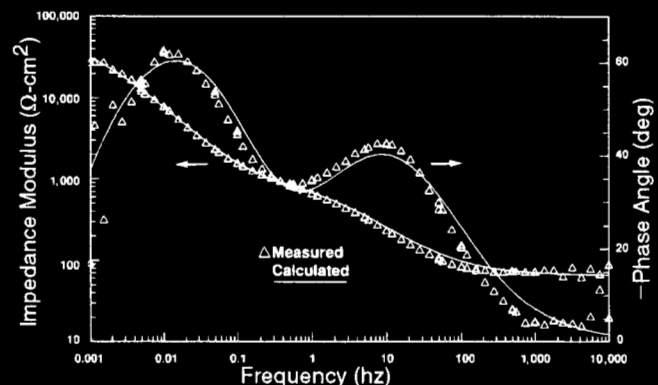


FIGURE 4. Impedance spectrum of steel in solution containing  $7.5 \times 10^{-3} M$  aspartate ion at  $90^\circ C$ , pH = 10, and 200 rpm after 24 h of exposure (Bode format).

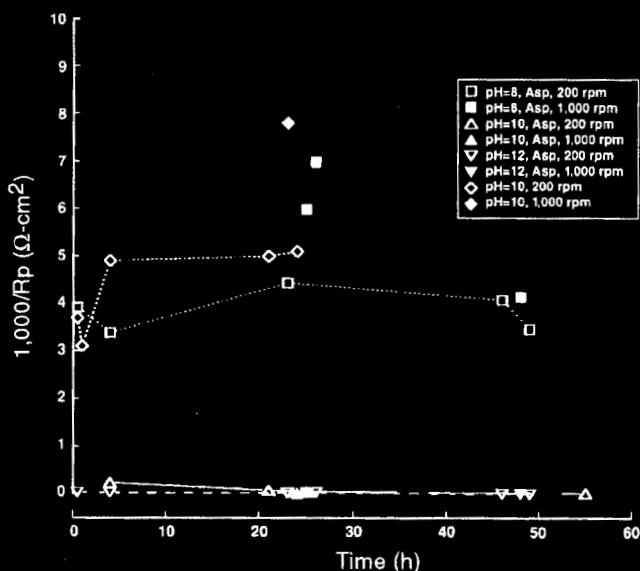


FIGURE 5. Plot of the reciprocal of the resistance used for estimating corrosion rates in Table 1 vs time. Reciprocal was multiplied by 1,000 for convenience. (Asp =  $C_4H_7NO_4$ ).

TABLE 1  
Comparison Between Corrosion Rates –  
Impedance vs Mass Loss at 90°C<sup>(A)</sup>

Conditions	Corrosion Rate (mm/y)	
	Impedance	Mass Loss
pH = 8 with sodium aspartate	2.8	2.3
pH = 10 with sodium aspartate	$4.1 \times 10^{-2}$	$6.8 \times 10^{-1}$
	$2.1 \times 10^{-2}$	$3.0 \times 10^{-2}$
pH = 10 without sodium aspartate	2.5	1.4
pH = 12 without sodium aspartate <sup>(B)</sup>	$1.2 \times 10^{-2}$	$1.4 \times 10^{-1}$

<sup>(A)</sup> The experiment at pH = 10 was repeated. All pH were as measured at 25°C (room temperature).

<sup>(B)</sup> There was seepage of liquid behind the spacer, which led to excess corrosion in the area not exposed directly to the fluid. This corrosion led to excess mass loss. The impedance estimate to be the more accurate measure of the time averaged corrosion rate.

TABLE 2  
Corrosion of Steel in L-Aspartic Acid at 30°C

pH @ 25°C	Concentration (molality)	Corrosion Rate (mm/y)	Comments
10.0	0.0	0.26	Uniform corrosion
10.3	$2.3 \times 10^{-1}$	< 0.0025	No attack

The pH boundary between high and low corrosion suggested by Figures 1 through 5 was very sharp. At a pH of ~10 as measured at 25°C (9 at 90°C), there was virtually no corrosion as long as the concentration of  $C_4H_7NO_4$  was high enough to completely inhibit the surface. However, at a pH of ~9.5 as measured at 25°C (8.3 at 90°C),  $C_4H_7NO_4$  offered no corrosion resistance. At this pH and lower, the corrosion rate seemed to be accelerated over that observed when  $C_4H_7NO_4$  was not present, in agreement with previous work at room temperature.<sup>3</sup>

While  $7.5 \times 10^{-3}$  M  $C_4H_7NO_4$  was an adequate concentration to impart complete corrosion inhibition under conditions of continuous fluid motion (Figures 2 through 4), under the more static conditions of the immersion experiments, higher concentrations were required. At the lower concentrations, areas of localized corrosion surrounded by larger areas of no corrosion were evident, with the effect decreasing with increasing  $C_4H_7NO_4$  concentration.

These observations suggested fluid motion enhanced corrosion inhibition of  $C_4H_7NO_4$  under basic conditions so that lower concentrations of the inhibitor were needed. This enhancement effect of corrosion inhibitors for steel in neutral and alkaline solutions with fluid motion has been observed previously with respect to nitrites and chromates.<sup>17</sup>

Whether a polymerized form of  $C_4H_7NO_4$  (polyaspartic acid) would act in a manner similar to the monomer was considered. Polyaspartic acid is formed by a linkage between the amine group of one molecule and the carboxylic acid group of another. Either carboxylic acid group can be involved. This linkage effectively removes one of the two carboxylic acid groups and possibly one of the pK values. Table 4 shows the results of immersion at 90°C for polyaspartic acid. Results showed again that there was a pH boundary. Above ~pH 10 as measured at room temperature, there was virtually no corrosion. Below that value, there was significant corrosion. The corrosion rate at pH = 8 was greater than that shown in Table 3 in the absence of polyaspartic acid.

## DISCUSSION

As shown by Figures 2 through 4 and Tables 1 through 3, the effect of pH on the corrosion inhibition properties of sodium aspartate with respect to Fe was dramatic. There was a change in mechanism at a pH between 9.5 and 10.0 as measured at 25°C (8.3 and 8.7 as measured at 90°C) independent of whether the additive was sodium aspartate or sodium polyaspartate. The measured pK of the most basic acid-base constant for  $C_4H_7NO_4$  at 25°C ranged between 9.59 and 10.06<sup>6</sup>. This coincidence of values strongly suggested the change in behavior was a result of the

**TABLE 3**  
Corrosion of Steel in L-Aspartic Acid at 90°C

pH @ 25°C (pH @ 90°C)	Concentration (molality)	Corrosion Rate (mm/y)	Comments
8.0 (7.1)	0.0	0.31	Severe general corrosion.
8.1 (7.3)	$7.5 \times 10^{-3}$	0.43	Uniform corrosion. Second sample > 0.63 mm/y
9.5 (8.3)	$2.3 \times 10^{-1}$	0.91	Significant general corrosion.
10.0 (8.7)	0.0	0.54	Severe general corrosion.
10.0 (9.1)	$7.5 \times 10^{-3}$	— <sup>(A)</sup>	Several deep craters. Large areas of no attack and shiny metal.
9.9 (8.9)	$3.8 \times 10^{-2}$	— <sup>(A)</sup>	One deep crater where coupon was held. Shiny metal elsewhere.
10.2 (9.1)	$7.5 \times 10^{-2}$	< 0.0025	One small area of etch. No attack elsewhere.
10.2 (9.1)	$2.3 \times 10^{-1}$	< 0.0025	No attack.
12.0	0.0	0.01	Some stains and etch.
11.1 (10.1)	$2.3 \times 10^{-1}$	< 0.0025	No attack.
13.1 (11.6)	$2.3 \times 10^{-1}$	< 0.0025	No attack.

<sup>(A)</sup> No corrosion rate was calculated because of the few areas of localized corrosion surrounded by significant areas of no corrosion.

solution pH crossing the pK of that acid-base constant. A fully ionized aspartate molecule was necessary for corrosion inhibition. The result also suggested this ionization constant was not affected by the loss of a carboxylic acid group upon creation of the polyaspartic acid molecule.

The potential-pH diagram suggested an hypothesis for this behavior. Interfacing the diagram with reality required placing the steady-state corrosion potential ( $E_{\text{corr}}$ ) and pH coordinate on the plot. This procedure assumed these values approximated the equilibrium potential and hydrogen ion activity (Figures 1[a] and [b]).

$E_{\text{corr}}$  for Fe changed by several hundred millivolts above and below the pH equal to the highest pK. As shown on the solid species diagram, at pH values below that pK,  $E_{\text{corr}}$  was in the region of stability of the dissolved iron-aspartate adduct. At pH values above

that pK,  $E_{\text{corr}}$  moved toward or remained in the region of stability of  $\text{Fe}_2\text{O}_3$ . The species iron oxyhydroxide ( $\text{FeOOH}$ ) was not included in these diagrams but would have been about as stable as  $\text{Fe}_2\text{O}_3$ .<sup>16</sup> At a pH of 9.0 to 9.1 at 90°C (~ 10 at 25°C),  $E_{\text{corr}}$  was near the boundary between the iron-aspartate adduct and  $\text{Fe}_2\text{O}_3$ . This pH was very near to that pH which demarcated the boundary between sodium aspartate acting as a corrosion accelerator and a corrosion inhibitor. The change in behavior was suggested to be caused by the stable form of Fe in the presence of  $\text{C}_4\text{H}_7\text{NO}_4$  changing from a dissolved adduct to an oxidized solid. The presence of  $\text{C}_4\text{H}_7\text{NO}_4$  was required for the transformation of the surface to occur so that inhibition occurred. This conclusion was supported by the fact that  $E_{\text{corr}}$  was about 300 mV more active at a pH of 10 and in the absence of  $\text{C}_4\text{H}_7\text{NO}_4$  than in its presence ( $-0.38 \text{ V}_{\text{SHE}}$  vs  $-0.06 \text{ V}_{\text{SHE}}$ ). Corrosion

**TABLE 4**  
*Corrosion of Steel in Polyaspartic Acid at 90°C*

pH @ 25°C (pH @ 90°C)	Molality of Repeat Units	Corrosion Rate (mm/y) <sup>(A)</sup>	Comment
8.0 (6.5)	2.3 x 10 <sup>-1</sup>	3.88	Almost uniform corrosion.
10.3 (8.7)	1.43 x 10 <sup>-2</sup>	— <sup>(A)</sup>	Some very shallow pits and one crater. Most of surface had no attack.
10.1 (8.4)	2.3 x 10 <sup>-1</sup>	< 0.0025	Virtually no attack.
9.6 (8.4)	2.6 x 10 <sup>-1</sup>	< 0.0025	Virtually no attack.

<sup>(A)</sup> No corrosion rate was calculated because of the few areas of localized corrosion surrounded by significant areas of no corrosion.

**TABLE 5**  
*Electrochemical Impedance Results for Steel In Sodium Aspartate at 90°C  
(Effect of Precorrosion on Corrosion Inhibition Properties)*

Exposure Time (h)	Rotation Rate (rpm)	Resistance (Ω-cm <sup>2</sup> )	Corrosion Rate by Mass Loss (mm/y)
<b>Precorroded at 90°C in Deionized Water Adjusted to pH = 5.75</b>			
5 to 7	200	2.4 x 10 <sup>2</sup>	1.8
17 to 19	200	8.7 x 10	(2.1 mm/y)
21	1,000	1.8 x 10 <sup>2</sup>	by impedance)
<b>Immersed Electrode in 5,000 ppm Aspartate Ion (pH = 9.91 at 25°C)</b>			
0.5	200	6.1 x 10 <sup>2</sup>	Not determined.
4 to 6	200	1.5 x 10 <sup>3</sup>	No iron detected in
19 to 21	200	3.0 x 10 <sup>3</sup>	solution by inductively
22	1,000	5.4 x 10 <sup>3</sup>	coupled plasma.
24	2,000	1.9 x 10 <sup>4</sup>	
42 to 44	200	6.0 x 10 <sup>3</sup>	
45	1,000	> 1.0 x 10 <sup>4</sup>	

resistance may have been caused by the C<sub>4</sub>H<sub>7</sub>NO<sub>4</sub> stabilizing the steel surface as an oxide, possibly Fe<sub>2</sub>O<sub>3</sub> or a form of FeOOH. As shown in Figure 1(b), the dissolved species at the higher pH probably was dominated by Fe(OH)<sub>4</sub><sup>-</sup>, but some dissolved form of iron aspartate may have been present.

Immersion results (Tables 2 and 3) supported the concept of the inhibition mechanism being one of oxidation of the surface because a sufficient concentration of sodium aspartate had to be present in solution for enough to adsorb to fully passivate the surface. If the concentration was deficient, some areas of the surface probably did not adsorb enough inhibitor to be passivated. These areas tended to become active relative to other areas where sodium aspartate was adsorbed. This difference in adsorption resulted in localized areas of extreme corrosion surrounded by

large areas of no corrosion. At these pH values, the steel surface region was a three-dimensional oxide.<sup>18</sup> Very likely, the sodium aspartate was incorporated into or reacted with the surface region to passivate it. This effect of inhibitor concentration has been noted with other inhibitors that incorporate in and oxidize a three-dimensional surface.<sup>10</sup> The beneficial effect of fluid motion observed in the present work also has been observed for inhibitors that tend to oxidize Fe surfaces.

Table 4 shows polyaspartic acid has corrosion inhibition properties similar to C<sub>4</sub>H<sub>7</sub>NO<sub>4</sub>. Polymerization eliminates one of the two carboxylic acid groups from each molecule. This suggested corrosion inhibition at high pH did not depend on two carboxylic acid groups being fully ionized on each moiety. The observation also suggested each aspartate moiety had to be ionized fully for the surface to become oxidized.

An inhibitor generally should be capable of passivating a precorroded metal surface. This ability was examined in the present study by precorroding a steel specimen and immersing the specimen in a solution containing  $3.8 \times 10^{-2}$  M (5,000 ppm) aspartate ion. The corrosion rate was estimated by EIS using the RCE in the same manner as described previously. Two relaxation time constants (constant-phase elements) were observed (Table 5).

Results suggested strongly that the aspartate ion did not have to interact with a clean Fe surface to decrease the corrosion rate of Fe. A comparison of Tables 2 and 5 indicated the corrosion rate decreased by  $\sim 1$  order of magnitude relative to what it would have been at pH of 10 in the absence of the inhibitor. The rate was  $\sim 0.54$  mm/y in the absence of inhibitor and  $\sim 0.05$  mm/y in the presence of inhibitor. This estimate assumed the resistance was  $\sim 5,000 \Omega\text{-cm}^2$ . The Tafel constant was  $\sim 0.025$  V for the precorroded surface.  $E_{\text{corr}}$  in the absence of aspartate at a pH of 10 was  $\sim -0.365$  V<sub>SHE</sub> ( $-0.625$  V<sub>Hg-Hg<sub>2</sub>Cl<sub>2</sub></sub>). In the presence of aspartate but with precorrosion of the surface, the potential was  $\sim -0.06$  V<sub>SHE</sub> ( $-0.32$  V<sub>Hg-Hg<sub>2</sub>Cl<sub>2</sub></sub>). The latter value was similar to that shown in Figure 1 for a noncorroded specimen. Thus, aspartate ion oxidized even a precorroded surface at high pH.

Amino acids of low molecular weight, other than C<sub>4</sub>H<sub>7</sub>NO<sub>4</sub>, exhibit this high-pH corrosion inhibition phenomenon.<sup>7</sup> C<sub>2</sub>H<sub>5</sub>O<sub>2</sub>N and C<sub>5</sub>H<sub>9</sub>O<sub>4</sub>N have been shown to exhibit similar characteristics with low corrosion rates found in solutions with pH  $\geq 10$  (as measured at 25°C) and a much higher corrosion rate in solutions at lower pH. Both of these amino acids have highest acid-base pK values of  $\sim 10$ .<sup>6</sup>

## CONCLUSIONS

❖ The ability of amino acids of low molecular weight, such as C<sub>4</sub>H<sub>7</sub>NO<sub>4</sub>, to inhibit the corrosion rate of Fe was shown to depend on pH of the solution. Only at

high pH was the corrosion rate reduced significantly. The pH boundary at which corrosion inhibition occurred was approximately equal to the most basic acid-base constant of the acid. The fully ionized form of C<sub>4</sub>H<sub>7</sub>NO<sub>4</sub> was required.

❖ The  $E_{\text{corr}}$  profile as a function of pH when placed on a potential-pH diagram suggested inhibition was caused by the most stable form of Fe changing from a dissolved iron-aspartate complex at lower pH to an oxide of Fe (possibly Fe<sub>2</sub>O<sub>3</sub> or FeOOH) at higher pH.

❖ Corrosion inhibition by polyaspartic acid demonstrated the same dependence on pH as inhibition by C<sub>4</sub>H<sub>7</sub>NO<sub>4</sub>.

## REFERENCES

1. A.J. Freedman, "Cooling Water Treatment," in *Process Industries Corrosion*, Vol. 8., eds. J. Moniz, W.J. Pollock (Houston, TX: NACE, 1986), p. 205.
2. V. Hluchan, B.L. Wheeler, N. Hackerman, *Werkst. Korros.* 39 (1988): p. 512.
3. R. Ramakrishnaiah, *Bull. Electrochem.* 2,1 (1986): p.7.
4. Nippon Rokoh Seishi, "Corrosion Inhibitor for (non) Ferrous Metals - Contains Amines and Amino Acids or Their Salts," Japanese Patent No. J50091546-A, July 22, 1975.
5. G.W. Whitman, R.P. Russell, V.J. Altieri, *Ind. & Eng. Chem.* 16, 7 (1924): p. 665.
6. L.G. Sillen, A.E. Martell, *Stability Constants of Metal-Ion Complexes*, Supplement No. 1, The Chemical Society (London, U.K.: Burlington House, 1971), p. 240.
7. D.J. Kalota, D. C. Silverman, "Process for Corrosion Inhibition of Ferrous Metals," U.S. Patent 4,971,724, issued Nov. 20, 1990.
8. D.C. Silverman, J. E. Carrico, *Corrosion* 44, 5 (1988): p. 280.
9. D.C. Silverman, *Corrosion* 40, 5 (1984): p. 220.
10. D.C. Silverman, "Corrosion Prediction from Circuit Models - Application to Evaluation of Corrosion Inhibitors," in *Electrochemical Impedance: Analysis and Interpretation*, ASTM STP 1186, eds. J. R. Scully, D.C. Silverman, M.W. Kendig (Philadelphia, PA: ASTM, 1993), p. 192.
11. D.C. Silverman, *Corrosion* 44, 9 (1988): p. 606.
12. A. Albert, *Biochemical J.* 50 (1952): p. 690.
13. D.D. Perrin, *J. Chem. Soc.* (1958): p. 3,125.
14. D.D. Perrin, *J. Chem. Soc.* (1959): p. 290.
15. D.C. Silverman, "Derivation and Application of EMF-pH Diagrams," in *Electrochemical Techniques for Corrosion*, ed. R. Baboian (Houston, TX: NACE, 1987), p. 117.
16. D.C. Silverman, *Corrosion* 38, 8 (1982): p. 453.
17. A. M. Shams El Din, A. M. R. Tag El Din, E. A. El Sum, *Metallurg. Corrosion-Industrie* 63, 752 (1988): p. 123.
18. W.J. Lorenz, F. Mansfeld, *Electrochim. Acta* 31, 4 (1986): p. 467.

## 1994 Author's Guide



# THE JOURNAL OF SCIENCE AND ENGINEERING CORROSION

A free 16-page guide for the prospective *CORROSION* author, with tips on manuscript preparation, format, style, and editorial policies.

To order, contact: NACE Membership Services Department  
P.O. Box 218340, Houston, TX, 77218-8340,  
713/492-0535, ext. 81, or FAX 713/579-6694.  
Item No. 32143